(11) S. Q. A. Rizvi, B. D. Gupta, W. Adcock, D. Doddnel and W. Kitching, *J. Organometal. Chem.*, **63**, 67 (1973).
(13) C. S. Chundy, M. F. Lapport and T. R. Spalding, *J. Chem. Soc. Dalton*, 558 (1976).
(14) A. Padwa, *Tetrahedron Lett.*, 3456 (1964); S. G. Cohen and R. J. Baumgarten, *J. Amer. Chem. Soc.*, **87**, 2996 (1965); C. Walling and M. J. Gibian, *ibid.*, **87**, 3361 (1965); R. Okazaki, K. Tamura, Y. Hirabayashi and N. Inamoto, *J. Chem. Soc. Perkin Trans.*, **1**, 1924 (1976).
(15) S. H. Band and I. M. T. Davison, *Trans. Faraday Soc.*, **66**, 406 (1970); A. Hosomi and H. Sakurai, *J. Amer. Chem. Soc.*, **94**, 1384 (1972); *ibem, Chem. Lett.*, 193 (1972); H. Sakurai, "Free Radicals," Ed. by J. K. Kochi, Vol. 2, Chapter 25, John Wiley & Sons, New York, 1973.
(16) H. Gilman and W. H. Atwell, *J. Amer. Chem. Soc.*, **86**, 5589 (1964).

Molecular Orbital Calculation for Polymeric Beryllium Hydride, Polyeihylene and Polymeric Boron Hydride According to the Pseudo-Lattice Method

Seok Heon Oh, Man Chai Jhang and Mu Shik Jhon

Department of Chemistry, Korea Advanced Institute of Science and Technology, P. O. Box 150 Chongyangni, Seoul 131, Korea (*Received August 24, 1983*)

The pseudolattice calculations in the CNDO/2 level of approximation are carried out for polymeric beryllium hydride, polyethylene and polymeric boron hydride. Since there is no evidence on the geometry for polymeric boron hydride, the two possible geometries are assumed. One is a polyethylene-type geometry and the other is a polymeric beryllium hydride-type geometry. In order to compare their relative stability, we calculate polyethylene and polymeric beryllium hydride and then compare with polymeric boron hydride having the assumed structures. The total energy calculation indicates that a polymeric beryllium hydride-type geometry is more stable than a polyethylene-type geometry. Our results obtained for polyethylene are in good agreement with those given by CNDO/2 crystal orbital. From the convergence problem with respect to the number of unit cells (M), the calculation with value of 4 for M can be considered to give the convergence limit results.

Introduction

The molecular orbital methods at various levels have been used to discuss the conformational energy of "polymers" by starting with the monomer and adding monomer unit one by one.[1]

Even though one can make a guess for a high-molecular weight polymer by continuing this process, the calculation becomes prohibitively difficult as the polymer grows and one never reaches a really large polymer. The polymer has been assumed to be an infinite chain of monomers having translational symmetry. Hence, the pseudolattice method can be also applied to polymeric systems.

In this study, polyethylene, polymeric beryllium hydride and polymeric boron hydride are adopted as model compounds for polymeric systems.

As a first example for our model studies, the polymeric beryllium hydride is treated. Because of experimental difficulties the structure of polymeric beryllium hydride has not yet been determined. It has been suggested[2] that a hydrogen bonded polymer might be a conceivable structure which could exist in polymeric beryllium hydride. Recent quantum mechanical calculations[3] supported this point of view.

Next, we employed the experimental result[4,5] that polyethylene is planar zig zag in the single crystal. Polyethylene has been studied by the *ab initio* MO method[6,7] and CNDO/2 crystal orbital.[8-14] Our MO calculation using the pseudolattice method is performed and compared with that of CNDO/2 crystal orbital.

Finally, polymeric boron hydride is chosen. This model is assumed to have the two possible geometries.

In order to determine the relative stability of these two possible geometries, MO calculations for both geometries are carried out and compared with each other. In this study, the coulomb lattice sums are involved in our MO calculations for polymeric system and becuase of computational limitation of *ab initio* method, CNDO/2 approximation[15-17] is used.

Theory

(*A*) *Pseudolattice method.* The pseudolattice method proposed by No and Jhon was applied to several ices[18] and solid HF.[19] In order to give the same environment for all molecules in a chosen cluster, overlap and coulomb integral matrices are composed of the submatrices which are obtained by making use of translational symmetry of molecules.

The pseudolattice method is therefore set up as follows.

(i) If the distances between two molecules is more larger than the interaction range considered (R_c), the overlap and coulomb integrals between the molecules are neglected. Hence, the matrix elements expressed in the atomic basis set can be written as follows.

$$F_{\mu n,\lambda m}=\langle x_\mu(r-R_n)|\hat{F}|x_\lambda(r-R_m)\rangle \quad (1)$$

$$S_{\mu n,\lambda m}=\langle x_\mu(r-R_n)|x_\lambda(r-R_m)\rangle \quad (2)$$

for $|R_n-R_m|<R_c$

and

$$F_{\mu n,\lambda m}=S_{\mu n,\lambda m}=0 \quad (3)$$

for $|R_n-R_m|>R_c$

where F is the one-electron Hartree-Fock operator and $S_{\mu n,\lambda m}$ is matrix elements of overlap integral. $\chi_\mu(r-R_n)$ is the atomic orbital centered on each site n, where $\mu=1, 2, \cdots\cdots\sigma$ denotes the atomic basis function (1S, 2S, $2P_x$, $2P_y$, $2P_z$).

(ii) Using the translational symmetry of molecules in a crystal or the polymeric system (not a translational symmetry of unit cell), the molecules located at the boundary of the model are translated to the nearest position of the other boundary molecules.

(B) Long-Range Coulomb Interaction. The long-range Coulomb interaction can be considered by calculating the coulomb lattice sums. The basic equations for the LCAO-SCF Hartree-Fock matrix in the CNDO/2 approximation can be written as follows.

$$F_{\mu\mu}=-\frac{1}{2}(I_\mu+A_\mu)+[(P_{AA}-Z_A)-\frac{1}{2}(P_{\mu\mu}-1)]\gamma_{AA}+\sum_{B(\neq A)}(P_{BB}-Z_B)\gamma_{AB} \quad (4)$$

$$F_{\mu\nu}=\beta_{AB}{}^{\circ}S_{\mu\nu}-\frac{1}{2}P_{\mu\nu}\gamma_{AB} \quad (5)$$

Where the atomic orbital X_μ belongs to atom A and χ_ν to atom B. $-1/2(I_\mu+A_\mu)$ is Mulliken-type atomic electronegativity, P_{AA} is the total charge density on atom A, $P_{\mu\nu}$ is a density matrix, Z_A is a core charge of the neutral atom A, and γ_{AB} is an average electrostatic repulsion between any electron on A and any electron on B.

For large interatomic distances, γ_{AB} will be approximately equal to R_{AB}^{-1} so that the last terms in Eq. (4) becomes as follows.

$$\sum_{B(\neq A)}(P_{BB}-Z_B)\gamma_{AB}=\left[\sum_{B(\neq A)}^{m}(P_{BB}-Z_B)\gamma_{AB}+\sum_{B>m}^{crystal}(P_{BB}-Z)R_{AB}^{-1}\right] \quad (6)$$

Where m denotes the maximal interaction atom. The last term in Eq. (6) is called the coulomb lattice sums and pre viously is taken by Bacon and Santry[20] in the perturbation approach.

Since coulomb lattice sums are added to $F_{\mu\mu}$, the new corresponding total energy can be expressed as follows.

$$\varepsilon_{total}=\frac{1}{2}\sum_{\mu\nu}P_{\mu\nu}(H_{\mu\nu}+F_{\mu\nu}^{*})+\sum_{A<B}\frac{Z_AZ_B}{R_{AB}}+\sum_A\varepsilon_{crystal} \quad (7)$$

$F_{\mu\nu}^{*}$ denotes a Fock matrix elements except coulomb lattice sums. Energy terms in the total energy expression are associated with one or two atoms in CNDO/2 calculation, so that an energy breakdown into monoatomic and diatomic contribution is possible.

$$\varepsilon_{total}=\sum_A\varepsilon_A+\sum_{A<B}\varepsilon_{AB}+\sum_A\varepsilon_{crystal} \quad (8)$$

The detailed expressions for ε_A and ε_{AB} are;

$$\varepsilon_A=\sum_\mu^A P_{\mu\mu}U_{\mu\mu}+\frac{1}{2}\sum_\mu^A\sum_\nu^A\left(P_{\mu\mu}P_{\nu\nu}-\frac{1}{2}P_{\mu\nu}^2\right)\gamma_{AA} \quad (9)$$

$$\varepsilon_{AB}=\sum_\mu^A\sum_\nu^B\left(2P_{\mu\nu}\beta_{\mu\nu}-\frac{1}{2}P_{\mu\nu}{}^2\gamma_{AB}\right)+(Z_AZ_BR_{AB}^{-1}-P_{AA}V_{AB}-P_{BB}V_{BA}+P_{AA}P_{BB}\gamma_{AB}) \quad (10)$$

For large intermolecular separations, the potential V_{AB}, V_{BA} and γ_{AB} are approximately equal to R_{AB}^{-1} so that the last group of terms in Eq. (10) becomes $Q_AQ_BR_{AB}^{-1}$, where Q_B is the net charge on atom B. This shows that the coulomb lattice sums provide a very efficient way of taking into account the electrostatic interaction between the charged atom. The energy of crystal field can be therefore expressed as follows.

$$\sum_A\varepsilon_{crystal}=\sum_A\frac{1}{2}\sum_{B>m}^{crystal}Q_AQ_BR_{AB}^{-1} \quad (11)$$

Calculation

MO calculations using the pseudolattice method for selected polymeric systems are carried out in order to determine the stabilities of the possible geometries and to test the convergence problem with respect to the number of unit cells (M). The total energy per unit cell and atomic charge densities are calculated as the function of the number of the cells (M) interacting with the origin cell.

The pseudolattice method involving coulomb lattice sums on polymeric systems have been performed for various numbers of the cells (M), M = 2, 3, 4, and 5. In order to investigate the effect of cut-off range of coulomb lattice sums on the total energy and atomic charge, MO calculations are performed for three different cut-off ranges.

The geometries adopted for three polymeric systems are as follows.

(A) Polymeric Beryllium Hydride. The most likely geometry is that of a linear chain of beryllium atoms linked by bridging hydrogen atoms tetrahedrally disposed around the beryllium atoms as shown in Figure 1. The beryllium 2P slater type-Orbital (STO) exponent employed the optimum value. The hydrogen atom 1S STO exponent and the beryllium-hydrogen interatomic distance are also taken from the optimized vlaue. The optimum value[21] of the three parameters were:

Be_{2P}, 1.114; R_{Be-H}, 1.345(Å); H_{1S}, 1.143.

The angle of H-Be-H is set at a bond angle of 90 °.

(B) Polyethylene. The elementary cell and molecular geometry chosen for polyethylene are shown in Figure 2. The planar trans extended geometry is considered and bond angles HCH and CCC are taken as 110° and 112°, respectively from the experimental data.[22,23] The C-C and C-H distances are

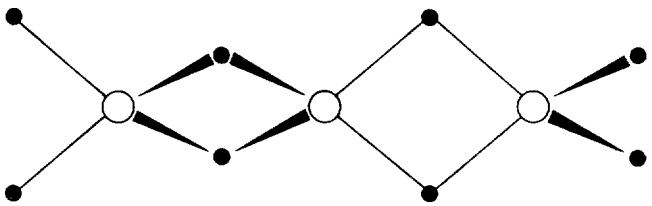

Figure 1. The geometry of polymeric beryllium hydride ($[(BeH_2)_2]_n$) Large open circles correspond to the beryllium atom, small full circles to the hydrogen atom.

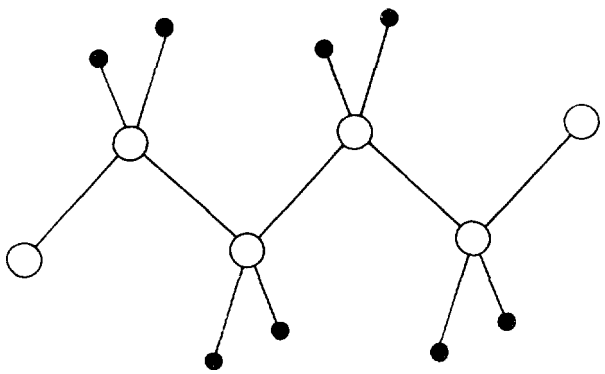

Figure 2. The geometry of polyethylene in all-*trans* zig zag conformation ($[(CH_2)_2]_n$). Large open circles correspond to the carbon atom, small full circles to the hydrogen atom.

fixed at 1.54Å and 1.09Å, respectively.

(*C*) *Polymeric boron hydride* Two possible geometries are assumed. First, a polyethylene-type geometry is employed, with all the interbond angles set at 110°and B–H bond lengths at 1.195Å. The B–B bond length is 2.25Å. In the second geometry, the bridging hydrogen bonds are assigned length 1.329Å in a model identical to the one employed for polymeric beryllium hydride. A HBH angle is set at 80 °.

Results and Discussions

In order to determine the more suitable of two possible geometries, MO calculations for both possible geometries of polymeric boron hydride are performed and these results are represented in Table 1 and 2. From our calculations, it is found that the bridging-hydrogen bond model is more stable than the polyethylene-type model.

The electronic structure of the BH_2 polymer poses an interesting question with respect to the linear polymeric beryllium hydride of similar geometry. If the band topology are basically the same, the extra two electrons given by boron would have to occupy the first degenerate pair of conduction bands, thus giving a linear metal.

The Mulliken population analysis for the wave function of both polymeric boron hydride are given in Table 2. In the case of the bridging-hydrogen bond model, there is a small electron drift from the hydrogen to the boron atom and a relatively small electron population in boron $2P_x$ orbitals. This confirms the weak nature of the framework bonds. on the other hand, in the case of the polyethylene-type model, there is a small electron drift from the boron atom to the hydrogen. This shows the reversed tendency in comparison to that of the bridging-hydrogen bond model. That is, the electron distribution also supported our calculated result that the bridging-hydrogen bond model is more suitable. Next, in order to investigate the convergence problem for the polymeric system with respect to the number of unit cells (M), we also calculate polyethylene and polymeric beryllium hydride. Our MO calculation results for polymeric beryllium hydride are listed in Table 3. The total energy calculation shows that polymeric beryllium hydride is more stable than the monomer. The total

TABLE 1: MO Calculation Results for two Possible Geometries of Polymeric Boron Hydride[a]

Geometry	Total energy[b] per BH_2	Total charge density	
		B	H
Polyethylenetype	−5.1886	2.9826	1.0087
Polymeric Beryllium hydridetype	−5.3508	3.2490	0.8739

[a] With four cells ($M=4$) and coulomb lattice sums up to 80Å; [b] All values are expressed in units of atomic unit.

TABLE 2: Total Atomic Population Calculated for both Geometries of Polymeric Boron Hydride[a]

Atomic population	Geometry	
	Polyethylene-type	Polymeric beryllium hydride-type
B 2S	0.9755	0.6389
$2P_x$	0.6754	0.5805
$2P_y$	0.8814	0.7768
$2P_z$	0.4503	1.2528
total	2.9826	3.2490
H	1.0087	0.8739

[a] With four cells ($M=4$) and coulomb lattice sums up to 80Å.

TABLE 3: Total Energy per BeH_2 Calculated for oly Polymeric Beryllium Hydride

Number of unit cells (M)	Total energy per BeH_2[d]		
	a	*b*	*c*
1	−3.5798	−3.5798	−3.5798
2	−3.7582	−3.7582	−3.7582
3	−3.7769	−3.7769	−3.7769
4	−3.7752	−3.7752	−3.7752
5	−3.7755	−3.7755	−3.7755

[a] With coulomb lattice sums up to 70 Å; [b] With coulomb lattice sums up to 140 Å; [c] With coulomb lattice sums up to 210 Å; [d] All values are expressed in units of atomic unit.

TABLE 4: Total Energy of BeH_2 in Various Configurations

	Total energy
BeH_2(linear)	−3.5617
BeH_2(angular)	−3.0864
BeH_2(unit in polymer)	−3.7752

energy and atomic charge densities are calculated as the function of various numbers of unit cells (M). The results thus obtained indicates that four cells are enough to predict informations for infinite chains.

On comparing the total energy per unit cell of polymeric beryllium hydride with twice that of monomeric BeH_2, the energy of polymerization for molecules is large, so the polymer is more stable. The energy change in the hypothetical process BeH_2(linear)–BeH_2(angular)–BeH_2 (unit in polymer) are all calculated and listed in Table 4. This indicates that the linear-angular reorganization process is energetically unfavored. However, on the polymerization, this reorganization energy is more than offset by the new hydrogen bridges formed.

The Mulliken population analysis is presented in Table 5.

TABLE 5: Total Charge Density of Polymeric Beryllium Hydride

Number of unit cells	Total charge density					
	a		*b*		*c*	
	Be	H	Be	H	Be	H
1	1.4985	1.2508	1.4985	1.2508	1.4985	1.2508
2	2.1717	0.9141	2.1717	0.9141	2.1717	0.9141
3	2.2061	0.8969	2.2061	0.8969	2.2061	0.8969
4	2.1959	0.9021	2.1959	0.9021	2.1959	0.9021
5	2.1983	0.9008	2.1983	0.9008	2.1983	0.9008

[a,b] and [c] are the same notations used in Table 3.

TABLE 6: Total energy per CH_2 and the Total Charge Densities Calculated with Various Numbers of Cells (M) for Polyethylene in Fully All-*trans* Conformation

Number of unit cells (M)	Total energy per CH_2[c]		Total charge density			
	a	*b*	C		H	
			a	*b*	*a*	*b*
2	−8.6967	−8.6967	3.9917	3.9917	1.0042	1.0042
3	−8.6853	−8.6853	3.9872	3.9872	1.0064	1.0064
4	−8.6884	−8.6884	3.9872	3.9872	1.0064	1.0064
5	−8.6886	−8.6886	3.9871	3.9871	1.0064	1.0064

[a] With coulomb lattice sums up to 50 Å; [b] With coulomb lattice sums up to 100 Å; [c] All values are expressed in units of atomic unit.

The overall tendency is for donation to take place from the hydrogen to beryllium with a net charge of approximately 0.198e accumulating on the beryllium atom.

Surprisingly enough, a slightly higher total energy per BeH_2 is found in $[(BeH_2)_2]_3$. This could in principle be traced back to a not yet sufficiently converged total energy per unit cell.

M. O. calculation results for polyethylene in the fully extended all-trans zigzag conformation are presented in Table 6. The result reveals that four cells are enough to predict the accurate total charge densities.

The total charge densities of polyethylene in the all *trans* conformation are compared with those of the central methylene group of *n*-propane, *n*-pentane, and *n*-heptane in all *trans* states in Table 7. It is noteworthy that the charge density of the carbon atom of polyethylene is very close to that of *n*-heptane and not to *n*-propane and *n*-pentane.

As shown in Table 7 and 8, our result for polyethylene agrees extremly well with that of CNDO/2 crystal orbital. From the Table 6, the calculation with the value of 4 for M can be considered to give the converged total energy per CH_2.

On comparing with the results of pseudolattice method applied to several ices[18] and solid HF,[19] those of our study show a slower convergence. This may be the reason why the polymeric system has much more interactions through bondings.

The variation of the charge distribution with the number of cells is investigated similarly as that of total energy per CH_2. Our result shows $C^{\delta+}$–$H^{\delta-}$ with only a small charge separation. From our results, the efect of cut-off range of coulomb lattice sums on the total energy per unit cell and charge densities is negligibly small.

From the total energy calculations for three polymeric systems adopted, the total energy for the two possible geometries of polymeric boron hydride is similar to that of polymeric beryllium hydride and not to that of polyethylene. That is, the polymeric beryllium hydride-type geometry is more suitable than the polyethylene-type geometry.

Because of the computational limitation of the application of *ab initio* MO Method to the polymeric system, our calculations used the CNDO/2 approximation.

TABLE 7: The Electronic Structure of Polyethylene in Comparison with *n*-propane, *n*-pentane and *n*-heptane[a]

Compound	Reference	Total charge density	
		C	H
polyethylene	CNDO/2-CO[d]	3.9871	1.0065
polyethylene[c]	our study	3.9872	1.0064
n-propane[b]	CNDO/2-CO[d]	3.9753	1.0056
n-pentane[b]	CNDO/2-CO[d]	3.9815	1.0045
n-heptane[b]	CNDO/2-CO[d]	3.9874	1.0051

[a] Assumed to be in the all-*trans* conformation; [b] The values of the central methylene group of molecules; [c] With four cells (M=4); [d] Taken from reference 9.

TABLE 8: Comparison the Pseudolattice Method with CNDO/2-CO

Method	Tatal energy per CH_2	Total charge density	
		C	H
CNDO/2-Crystal Orbital	−8.6881[a]	3.9872[b]	1.0064[b]
Our result	−8.6884[c]	3.9872[c]	1.0064[c]

[a] With seven cells for the value of M (M=7); [b] With six cells (M=6); [c] With four cells (M=4)

Acknowledgement. This work was supported in part by Korea Research Center for Theoretical Physics and Chemistry

and Korea Science and Engineering Foundation.

References

(1) A. Rossi and C. W. David and R. Schor, *Theoret. Chim. Acta.*, **14**, 429 (1969).
(2) E. Wiberg and R. Bauer, *Z. Naturforsch.*, **6b**, 171 (1951).
(3) R. Ahlrichs and W. Kutzelnigg, *Theoret. Chim. Acta. (Berl)*, **10**, 377 (1968).
(4) P. H. Geil, "Polymer Single Crystals," Interscience, New York, 1963.
(5) H. D. Keith, "Physics and Chemistry of the Organic Solid State," Vol. I, Interscience, New York, 1963.
(6) J. M. Andre and G. Leroy, *Chem. Phys. Lett.*, **5**, 71 (1970).
(7) J. M. Andre, G. S. Kapsomenos and G. Leroy, *Chem. Phys. Lett.*, **8**, 195 (1971).
(8) J. M. Andre and J. Delhalle, *Chem. Phys. Lett.*, **17**, 145 (1972).
(9) K. Morokuma, *Chem. Phys. Lett.*, **6**, 186 (1970).
(10) H. Fujita and A. Imamura, *J. Chem. Phys.*, **53**, 4555 (1970).
(11) G. Morosi and M. Simonetta, *Chem. Phys. Lett.*, **8**, 358 (1971).
(12) K. Morokuma, *J. Chem. Phys.*, **54**, 1962 (1971).
(13) J. M. Andre, J. Delhale, G. S. Kapsomenos and G. Leroy, *Chem. Phys. Lett.*, **14**, 485 (1972).
(14) B. J. McAloon and P. G. Perkins, *Faraday Discuss.*, **II**, 1121 (1971).
(15) J. A. Pople, D. P. Santry and G. A. Segal, *J. Chem. Phys.*, **43**, S129, S136 (1965).
(16) J. A. Pople and G.A. Segal, *J. Chem. Phys.*, **44**, 3289 (1966)
(17) J. A. Pople and D. L. Boveridge, "Approxinate Molecular Orbital Theory," McGraw-Hill, New York (1970).
(18) K. T. No, and M. S. Jhon, *J. Phys. Chem.*, **87**, 226 (1983).
(19) J. S. Kim, K. J. No and M. S. Jhon, Sumitted to J. Phys. Chem.
(20) J. Bacon and D. P. Santry, J. Chem. Phys., **56**, 2011 (1972).
(21) R. David and G. Perkins, *Theoret. Chim. Acta.* (Berl), **51**, 163(1979).
(22) S. Kavesh and J. M. Schultz, *J. Polym. Sci., Part A-2*, **8**, 243(1970).
(23) T. Yemni and R. L. McCullough, *J. Polym. Sci., Part A-2*, **11**, 1385 (1973).

Kinetics and Mechanisms of the Oxidation of Carbon Monoxide on Ni-Doped α-Fe_2O_3

Keu Hong Kim, Jong Ho Jun and Jae Shi Choi

Department of Chemistry, Yonsei University, Seoul 120, Korea (*Received September 15, 1983*)

The oxidation of carbon monoxide has been investigated on Ni-doped α-Fe_2O_3 catalyst at 300 to 450 °C. The oxidation rates have been correlated with 1.5-order kinetics; first with respect to CO and 1/2 with respect to O_2. Carbon monoxide is adsorbed on lattice oxygen of Ni-doped α-Fe_2O_3, while oxygen appears to be adsorbed on oxygen vacancy formed by Ni-doping. The conductivities show that adsorption of CO on O-lattice produces conduction electron and adsorption of O_2 on O-vacancy withdraws the conduction electron from vacancy. The adsorption process of CO on O-lattice is rate-determining step and dominant defect of Ni-doped α-Fe_2O_3 is suggested from the agreement between kinetic and conductivity data.

Introduction

A classification of solid catalysts based on electronic properties was formally announced by Dowden.[1] This classification sorted out catalysts into three distinct groups: (a) Conductors (metals), (b) Semiconductors (metal oxides and sulphides) and (c) Insulators (refractory oxides). From the standpoint of widespread application as catalysts, extrinsic semiconductors, which owe their electrical conductance to defect lattice structure of nonstoichiometry or both, are of absorbing interest. Nonstoichiometry may arise out of the incorporation of extra atoms into the crystal at interstitial sites or due to the vacancies caused by the absence of atoms from normal sites. Oxygen vacancies in ZnO are due to excess Zn dissolved in the interstitial sites of ZnO.[2] On the other hand, oxygen deficiency in ZnO is due to excess Zn which can be dissolved in the interstitial sites of ZnO.[3-7]

The catalytic properties of a semiconductor, such as its specificity and activity for a particular reaction, are strongly dependent upon its electronic properties. This is strikingly demonstrated by the effect of doping on the electrical and catalytic properties of the semiconductor. The systematic studies of Schwab and Block[8] on the oxidation of CO on Li- and Cr-doped NiO and on Li- and Ga-doped ZnO provide suitable examples to illustrate this correlation.

On a α-Fe_2O_3 catalyst, it was reported that an Fe_i^{2+} interstitial and an oxygen vacancy might be required to adsorb CO and O_2[9]. Ni-doped α-Fe_2O_3, however, the catalyst used in this work shows that CO is adsorbed on lattice oxygen of Ni-doped α-Fe_2O_3, while O_2 appears to be adsorbed on